

# Constraints on relativity violations from gamma-ray bursts

V. Alan Kostelecký<sup>a</sup> and Matthew Mewes<sup>b</sup>

<sup>a</sup>*Physics Department, Indiana University, Bloomington, IN 47405, USA*

<sup>b</sup>*Physics Department, Swarthmore College, Swarthmore, PA 19081, USA*

(Dated: IUHET 572, January 2013)

## Abstract

Tiny violations of the Lorentz symmetry of relativity and the associated discrete CPT symmetry could emerge in a consistent theory of quantum gravity such as string theory. Recent evidence for linear polarization in gamma-ray bursts improves existing sensitivities to Lorentz and CPT violation involving photons by factors ranging from ten to a million.

Observations of photon behavior provide crucial probes of fundamental physics. Famous examples include the classic Michelson-Morley, Kennedy-Thorndike, and Ives-Stilwell experiments [1], which support the foundational Lorentz invariance of relativity. In recent years, a wide range of astrophysical, solar-system, and laboratory tests of Lorentz symmetry and its associated discrete CPT symmetry have achieved impressive sensitivities using photons (see Ref. [2] for a compilation). One motivation for these efforts is the prospect that tiny violations of these invariances could emerge in a consistent theory of quantum gravity such as string theory [3]. In this paper, we use recent measurements of linear polarization in light from gamma-ray bursts (GRB) [4–6] to improve existing sensitivities to a variety of Lorentz- and CPT-violating effects by factors ranging from ten to a million. The key to the exceptional GRB sensitivity to Lorentz and CPT violation lies primarily in the extreme propagation distances during which tiny effects can accumulate, along with the comparatively high photon energies involved.

At accessible energies, violations of Lorentz invariance are governed by the Standard-Model Extension (SME) [7], a comprehensive effective field theory containing both General Relativity and the Standard Model that provides a general theoretical framework for observational studies. This theory also describes CPT violation in the context of realistic field theory [8]. The SME action is a sum of coordinate-invariant terms, including ones formed from Lorentz-violating operators contracted with controlling coefficients, and the mass dimension  $d$  of each operator fixes the dimensionality of the corresponding coefficient [9]. In the photon sector, all gauge-invariant operators describing the propagation of light have been classified and enumerated for arbitrary  $d$  [10].

The SME predicts that light propagates in the presence of Lorentz and CPT violation as the superposition of two normal modes that may differ in speed and polarization. The dispersion relations connecting the photon energy  $E$  and momentum  $p$  for the two modes can be written in the compact but implicit form [7, 10]

$$E = (1 - \varsigma^0 \pm \sqrt{(\varsigma^1)^2 + (\varsigma^2)^2 + (\varsigma^3)^2})p, \quad (1)$$

where the dimensionless quantities  $\varsigma^a = \varsigma^a(E, \theta, \phi)$  depend both on  $E$  and on the photon direction of propagation, which for an astrophysical point source is fixed by the source codeclination  $\theta \equiv (90^\circ - \text{declination})$  and by the right ascension  $\phi$ . For light propagating *in vacuo*, the quantities  $\varsigma^a$  are linear combinations of the basic SME coefficients  $c_{(I)jm}^{(d)}$ ,  $k_{(E)jm}^{(d)}$ ,

$k_{(B)jm}^{(d)}$ , and  $k_{(V)jm}^{(d)}$ , where  $j, m$  are angular quantum numbers. For each  $d$ , many different SME coefficients control the behavior of light. A given point source at a fixed sky location can therefore access only a limited number of coefficient combinations. Consequently, multiple sources at different sky locations are required to constrain fully the coefficient space.

Two major features, dispersion and birefringence, can be exploited to search for Lorentz violation in radiation from sources at cosmological distances. Dispersion is a characteristic of all SME operators with  $d \neq 4$ . Arrival-time differences in high-energy photons from sources such as GRB can be used to constrain the energy dependence in the group velocity. The SME framework shows that dispersion for operators with odd  $d$  is necessarily accompanied by birefringence, implying different speeds for the two normal modes. As a result, a wave packet not only disperses but gradually splits into two. Only the CPT-even operators with even  $d$  characterized by the coefficients  $c_{(I)jm}^{(d)}$  give dispersion without birefringence. GRB constraints on Lorentz-violating dispersion for even dimensions  $d$  have been obtained for  $d = 6$  and  $8$  [10–13].

Birefringence studies of astrophysical sources such as GRB offer extreme sensitivity to Lorentz and CPT violation. The primary signature of birefringence is a change in photon polarization due to propagation. This is governed by the phase difference of the eigenmodes developed during propagation, which increases with energy. While dispersion can uniquely constrain the coefficients  $c_{(I)jm}^{(d)}$ , for  $d \geq 4$  birefringence at GRB energies typically offers many orders of magnitude better sensitivity to the coefficients  $k_{(E)jm}^{(d)}$ ,  $k_{(B)jm}^{(d)}$ ,  $k_{(V)jm}^{(d)}$  because a comparable dispersion test would require a time resolution comparable to the tiny inverse photon frequency.

In one study, evidence for polarization at the level of  $\Pi > 35\%$  in GRB 930131 and  $\Pi > 50\%$  in GRB 960924 was extracted from data obtained by the Burst and Transient Source Experiment (BATSE) [14]. These results have been used to constrain Lorentz violation for  $d = 4, 5, 6, 7, 8, 9$  [10, 15]. Polarization as high as  $\Pi = 96_{-40}^{+39}\%$  was identified in GRB 041219A using instruments aboard the International Gamma-Ray Astrophysics Laboratory (INTEGRAL) [4]. This result was used by Stecker to place bounds on  $d = 5$  coefficients on the order of  $10^{-34} \text{ GeV}^{-1}$  [16]. Another INTEGRAL analysis found similarly high degrees of polarization in GRB 041219A, placing bounds on the single isotropic  $d = 5$  coefficient [17]. A recent analysis using polarization data for GRB 100826A ( $> 6\%$ ), GRB 110301A ( $> 31\%$ ), and GRB 110721A ( $> 35\%$ ) from the Gamma-ray Burst Polarimeter (GAP) on

	$z$	energy	$(\theta, \phi)$
GRB 930131	0.1 [15]	31 – 98 keV [14]	$(98^\circ, 182^\circ)$ [19]
GRB 960924	0.1 [15]	31 – 98 keV [14]	$(87^\circ, 37^\circ)$ [19]
GRB 041219A	0.02 [17]	100– 1000 keV [4]	$(27^\circ, 6^\circ)$ [20]
GRB 100826A	0.71 [18]	70 – 300 keV [5]	$(112^\circ, 279^\circ)$ [21]
GRB 110301A	0.21 [18]	70 – 300 keV [6]	$(61^\circ, 229^\circ)$ [22]
GRB 110721A	0.45 [18]	70 – 300 keV [6]	$(129^\circ, 333^\circ)$ [23]

TABLE I: GRB for which strong evidence of linear polarization exists. The second column gives the estimated lower limit on the red shift. The third column is the energy range in which polarization is observed. The last column gives the GRB codeclination  $\theta$  and right ascension  $\phi$ . The first two GRB were previously studied [10, 15], while the others are the subject of the present work.

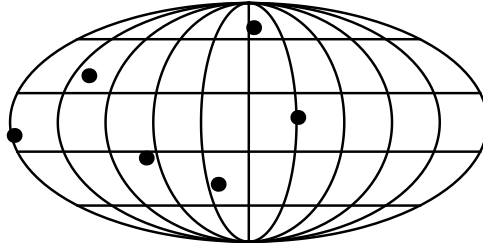


FIG. 1: Sky map showing the locations of the six GRB listed in Table I. The map is centered at  $(\theta, \phi) = (90^\circ, 0^\circ)$ .

the Interplanetary Kite-craft Accelerated by Radiation of the Sun (IKAROS) [5, 6] also bounded the single isotropic  $d = 5$  coefficient [18]. The basic features of all six GRB are summarized in Table I, and their celestial locations are displayed in Fig. 1.

In this work, we use the polarization reported for the four latest GRB to place improved bounds on direction-dependent combinations of SME coefficients for  $d = 4, 5, 6, 7, 8, 9$ . For the analysis, it is useful to expand the quantities  $\varsigma^a$  in energy  $E$  [10, 11],

$$\varsigma^a(E, \theta, \phi) = \sum_d E^{d-4} \varsigma^{(d)a}(\theta, \phi), \quad (a = 0, 1, 2, 3), \quad (2)$$

where  $\varsigma^{(d)a}(\theta, \phi)$  are direction-dependent combinations of SME coefficients. The direction dependence can be displayed explicitly by further expansion using conventional spherical

	coeff.	CPT	$d$	$j$	biref.
general	$c_{(I)jm}^{(d)}$	+	$4, 6, 8, \dots$	$0, 1, \dots, d-2$	
	$k_{(E)jm}^{(d)}$	+	$4, 6, 8, \dots$	$2, 3, \dots, d-2$	✓
	$k_{(B)jm}^{(d)}$	+	$4, 6, 8, \dots$	$2, 3, \dots, d-2$	✓
	$k_{(V)jm}^{(d)}$	-	$3, 5, 7, \dots$	$0, 1, \dots, d-2$	✓
isotropic	$c_{(I)00}^{(d)}$	+	$4, 6, 8, \dots$	0	
	$k_{(V)00}^{(d)}$	-	$3, 5, 7, \dots$	0	✓

TABLE II: Index ranges and properties of coefficients for Lorentz and CPT violation, where  $-j \leq m \leq j$  as usual. The isotropic limit is shown in the last two lines.

harmonics  $Y_{jm}(\theta, \phi)$  for  $\varsigma^{(d)0}(\theta, \phi)$  and  $\varsigma^{(d)3}(\theta, \phi)$ ,

$$\begin{aligned}
\varsigma^{(d)0}(\theta, \phi) &= \sum_{jm} Y_{jm}(\theta, \phi) c_{(I)jm}^{(d)}, \\
\varsigma^{(d)3}(\theta, \phi) &= \sum_{jm} Y_{jm}(\theta, \phi) k_{(V)jm}^{(d)},
\end{aligned} \tag{3}$$

and their cousins  ${}_{\pm 2}Y_{jm}(\theta, \phi)$  of spin-weight two for the combinations  $\varsigma^{(d)\pm} \equiv \varsigma^{(d)1} \mp i\varsigma^{(d)2}$ ,

$$\varsigma^{(d)\pm}(\theta, \phi) = \sum_{jm} {}_{\pm 2}Y_{jm}(\theta, \phi) (k_{(E)jm}^{(d)} \pm ik_{(B)jm}^{(d)}). \tag{4}$$

The basic SME coefficients  $c_{(I)jm}^{(d)}$ ,  $k_{(E)jm}^{(d)}$ , and  $k_{(B)jm}^{(d)}$  characterize CPT-preserving Lorentz violation, while  $k_{(V)jm}^{(d)}$  also controls CPT violation. Table II summarizes some properties of these coefficients.

Table II also contains information about the isotropic coefficients for which  $j = m = 0$ , which represent a popular restriction of the general framework. In this limit, each value of  $d$  has exactly one SME coefficient, which is nonbirefringent in the CPT-even case and birefringent in the CPT-odd case. The theoretical motivation for this restriction is open to doubt because isotropy can hold only in a single inertial frame, which cannot be an Earth-based frame and requires fine tuning to match the standard Sun-centered frame. However, the isotropic limit does offer an order-of-magnitude measure of the reach for a given source, and it also simplifies many equations. For example, the general expression for the defect in the group velocity relevant for dispersion studies can be written  $\delta v_{gr} = (d-3)E^{d-4}(-\varsigma^{(d)0} \pm |\varsigma^{(d)+}|)$  in the CPT-even case and  $\delta v_{gr} = \pm(d-3)E^{d-4}|\varsigma^{(d)3}|$  in

the CPT-odd case, but in the isotropic limit one obtains instead the simpler expressions  $\delta v_{gr} = -(d-3)E^{d-4}c_{(I)00}^{(d)}/\sqrt{4\pi}$  in the CPT-even case and  $\delta v_{gr} = \pm(d-3)E^{d-4}k_{(V)00}^{(d)}/\sqrt{4\pi}$  in the CPT-odd case. Note that Table II reveals there are no  $j = 0$  isotropic coefficients  $k_{(E)jm}^{(d)}$  or  $k_{(B)jm}^{(d)}$ , so the quantities  $\varsigma^{(d)\pm}$  are necessarily direction dependent.

During birefringent propagation of light, the difference in phase speed between the two normal modes generates a relative phase shift and a corresponding change in the net polarization. This change can be visualized as a rotation of the Stokes vector  $\vec{s} = (s^1, s^2, s^3) = (Q, U, V)$  about a rotation axis  $\vec{\varsigma} = (\varsigma^1, \varsigma^2, \varsigma^3)$  by an angle  $\Phi$  equal to the total relative phase shift [24]. If  $\vec{s}$  lies along  $\vec{\varsigma}$ , then the light is in one of the two normal modes and the polarization remains unchanged. Note that in the CPT-odd case the two normal modes are circularly polarized,  $\vec{\varsigma} = (0, 0, \varsigma^3)$ , while in the CPT-even case they are linearly polarized,  $\vec{\varsigma} = (\varsigma^1, \varsigma^2, 0)$ . Also, isotropic birefringence occurs only in the CPT-odd case where  $\varsigma^3 = E^{d-4}k_{(V)00}^{(d)}/\sqrt{4\pi}$  and for which  $d$  is odd, so changes in polarization for even  $d$  necessarily depend on the source position.

For given  $d$ , the rotation angle  $\Phi$  depends on the difference in phase speed,  $\Delta v = 2E^{d-3}|\varsigma^{(d)a}|$ , where  $a = 3$  in the CPT-odd case and  $a = +$  in the CPT-even case. It can be found by integrating the accumulated phase over the propagation time,  $\Phi = \int E\Delta v dt$ . Incorporating the redshift gives

$$\Phi = 2E^{d-3}L^{(d)}|\varsigma^{(d)a}(\theta, \phi)|, \quad a = (3, +), \quad (5)$$

where  $L^{(d)} = \int_0^z (1+z)^{d-4} H_z^{-1} dz$  is the effective baseline for dimension  $d$  in terms of the source redshift  $z$  and the Hubble expansion rate  $H_z$  at redshift  $z$ .

For the CPT-odd case with  $a = 3$ , the Stokes vector rotates about the  $s^3$  axis, shifting the linear polarization angle  $\psi$  by  $\delta\psi = \Phi/2$ . A detailed analysis searching for CPT violation could take advantage of the  $E^{d-3}$  dependence in Eq. (5). For example, assuming two photons of energies  $E_1$  and  $E_2$  initially have the same polarization, the difference  $\psi_2 - \psi_1$  in their polarization angles after traveling the effective baseline  $L^{(d)}$  is given by

$$\frac{\psi_2 - \psi_1}{(E_2^{d-3} - E_1^{d-3})L^{(d)}} = \sum_{jm} Y_{jm}(\theta, \phi) k_{(V)jm}^{(d)}. \quad (6)$$

Using observations of GRB 041219A and assuming only the single isotropic coefficient with  $d = 5$  [25], a search of this type was performed in Ref. [17], yielding the bound  $|k_{(V)00}^{(5)}| < 3 \times 10^{-33} \text{ GeV}^{-1}$ .

An alternative approach offering conservative constraints is to seek a significant degree of linear polarization within a given energy band. Differential rotations within the band smear the polarization and hence decrease the effective degree of linear polarization,  $\Pi_{\text{eff}} = \sqrt{\langle s^1 \rangle^2 + \langle s^2 \rangle^2}$ . In the CPT-odd case, this smearing produces an upper bound in the measured polarization  $\Pi \leq \sqrt{\langle \cos \Phi \rangle^2 + \langle \sin \Phi \rangle^2}$ , where the equality holds for an initial 100% linear polarization at constant angle. The polarization smearing will be nearly complete unless the change in  $\Phi$  over the energy band is less than  $2\pi$ . Under the assumption of only the single isotropic coefficient with  $d = 5$ , a similar idea has been applied to observations of GRB 100826A, GRB 110301A, and GRB 110721A [18], producing the bound  $|k_{(V)00}^{(5)}| < 6 \times 10^{-34} \text{ GeV}^{-1}$ .

In the general case, for any given odd  $d$  and including all coefficients for CPT violation, we obtain the conservative limit

$$\left| \sum_{jm} Y_{jm}(\theta, \phi) k_{(V)jm}^{(d)} \right| < \frac{\pi}{|E_2^{d-3} - E_1^{d-3}| L^{(d)}}, \quad (7)$$

where  $E_1$  and  $E_2$  are the edges of the energy band. This expression can be used to obtain substantially improved sensitivities to CPT violation from GRB 041219A, GRB 100826A, GRB 110301A, and GRB 110721A. We consider CPT-violating operators of dimensions  $d = 5, 7$ , and  $9$ , for which there are  $16, 36$ , and  $64$  independent vacuum coefficients, respectively [10]. Each source generates a new constraint on a different combination of coefficients, listed in Table III. For completeness, we also list bounds in the isotropic limit. These results represent improvements in sensitivity over existing limits on violations of CPT symmetry ranging from tenfold to about a millionfold.

The CPT-even case is more complicated because the normal modes are linearly polarized, which implies linearly polarized light from a distant source produced near one of the two polarizations  $\vec{s} \approx \pm(\varsigma^1, \varsigma^2, 0)$  could propagate essentially unchanged. Moreover, even if both modes are involved, the change in polarization involves more than a simple rotation of linear polarization. Light that is initially linearly polarized,  $\vec{s} = (s^1, s^2, 0)$ , becomes elliptically polarized as  $\vec{s}$  rotates out of the  $s^1$ - $s^2$  plane and in some cases may even become circularly polarized,  $\vec{s} = (0, 0, s^3)$ .

For light not produced in a normal mode and initially linearly polarized at angle  $\psi_0$ , let  $\Psi = \psi_0 - \psi_b$  be the difference between  $\psi_0$  and the polarization angle  $\psi_b$  for the faster of the two normal modes. As the Stokes vector rotates about  $\vec{\varsigma}$ , it traces out a cone with

	GRB 041219A (27°, 6°)	GRB 100826A (112°, 279°)	GRB 110301A (61°, 229°)	GRB 110721A (129°, 333°)
$ \sum_{jm} Y_{jm}(\theta, \phi) k_{(V)jm}^{(5)} $	$< 2 \times 10^{-34} \text{ GeV}^{-1}$	$< 7 \times 10^{-35} \text{ GeV}^{-1}$	$< 2 \times 10^{-34} \text{ GeV}^{-1}$	$< 1 \times 10^{-34} \text{ GeV}^{-1}$
$ \sum_{jm} Y_{jm}(\theta, \phi) k_{(V)jm}^{(7)} $	$< 2 \times 10^{-28} \text{ GeV}^{-3}$	$< 4 \times 10^{-28} \text{ GeV}^{-3}$	$< 2 \times 10^{-27} \text{ GeV}^{-3}$	$< 8 \times 10^{-28} \text{ GeV}^{-3}$
$ \sum_{jm} Y_{jm}(\theta, \phi) k_{(V)jm}^{(9)} $	$< 2 \times 10^{-22} \text{ GeV}^{-5}$	$< 2 \times 10^{-21} \text{ GeV}^{-5}$	$< 2 \times 10^{-20} \text{ GeV}^{-5}$	$< 5 \times 10^{-21} \text{ GeV}^{-5}$
$ k_{(V)00}^{(5)} $	$< 8 \times 10^{-34} \text{ GeV}^{-1}$	$< 2 \times 10^{-34} \text{ GeV}^{-1}$	$< 9 \times 10^{-34} \text{ GeV}^{-1}$	$< 4 \times 10^{-34} \text{ GeV}^{-1}$
$ k_{(V)00}^{(7)} $	$< 8 \times 10^{-28} \text{ GeV}^{-3}$	$< 1 \times 10^{-27} \text{ GeV}^{-3}$	$< 8 \times 10^{-27} \text{ GeV}^{-3}$	$< 3 \times 10^{-27} \text{ GeV}^{-3}$
$ k_{(V)00}^{(9)} $	$< 8 \times 10^{-22} \text{ GeV}^{-5}$	$< 7 \times 10^{-21} \text{ GeV}^{-5}$	$< 7 \times 10^{-20} \text{ GeV}^{-5}$	$< 2 \times 10^{-20} \text{ GeV}^{-5}$
$ \sum_{jm} 2Y_{jm}(\theta, \phi) (k_{(E)jm}^{(4)} + ik_{(B)jm}^{(4)}) $	$\lesssim 10^{-37}$	$\lesssim 10^{-38}$	$\lesssim 10^{-38}$	$\lesssim 10^{-38}$
$ \sum_{jm} 2Y_{jm}(\theta, \phi) (k_{(E)jm}^{(6)} + ik_{(B)jm}^{(6)}) $	$\lesssim 10^{-31} \text{ GeV}^{-2}$	$\lesssim 10^{-32} \text{ GeV}^{-2}$	$\lesssim 10^{-31} \text{ GeV}^{-2}$	$\lesssim 10^{-31} \text{ GeV}^{-2}$
$ \sum_{jm} 2Y_{jm}(\theta, \phi) (k_{(E)jm}^{(8)} + ik_{(B)jm}^{(8)}) $	$\lesssim 10^{-25} \text{ GeV}^{-4}$	$\lesssim 10^{-25} \text{ GeV}^{-4}$	$\lesssim 10^{-24} \text{ GeV}^{-4}$	$\lesssim 10^{-24} \text{ GeV}^{-4}$

TABLE III: New constraints on coefficients for Lorentz and CPT violation. The first three rows give constraints on general coefficients for CPT-odd operators with  $d = 5, 7, 9$ . The next three rows display constraints within the isotropic limit. The final three rows provide the approximate maximal sensitivity of each source to coefficients for CPT-even operators with  $d = 4, 6, 8$ .

opening angle  $4\Psi$  centered around  $\vec{\zeta}$ . A calculation shows that the difference  $\psi_2 - \psi_1$  in linear polarization at two different energies  $E_1$  and  $E_2$  satisfies

$$\begin{aligned} \sin 2(\psi_2 - \psi_1) &= \frac{\sin 2\Psi \cos 2\Psi (\cos \Phi_2 - \cos \Phi_1)}{\sqrt{(1 - \sin^2 2\Psi \sin^2 \Phi_1)(1 - \sin^2 2\Psi \sin^2 \Phi_2)}}, \\ \cos 2(\psi_2 - \psi_1) &= \frac{\cos^2 2\Psi + \sin^2 2\Psi \cos \Phi_2 \cos \Phi_1}{\sqrt{(1 - \sin^2 2\Psi \sin^2 \Phi_1)(1 - \sin^2 2\Psi \sin^2 \Phi_2)}}. \end{aligned} \quad (8)$$

This result could be used to place constraints when the observed difference  $\psi_2 - \psi_1$  is small.

An alternative and simpler strategy is again provided by considering the effective degree of linear polarization. In the CPT-even case, the effective degree of linear polarization is decreased both by polarization smearing and by the conversion from linear to elliptical polarization. The maximum effective degree of linear polarization is

$$\Pi_{\text{eff}} = \sqrt{1 - (1 - \langle \cos \Phi \rangle^2) \sin^2 2\Psi}. \quad (9)$$

An observation of linear polarization  $\Pi$  then places a lower limit on  $\Pi_{\text{eff}}$ , which leads to the inequality  $1 - \Pi^2 > (1 - \langle \cos \Phi \rangle^2) \sin^2 2\Psi$ . A single source therefore bounds a region in coefficient space but cannot provide a strict constraint, as its light could be propagating in a normal mode with  $\Psi = 0$  or  $\pi/2$ . In principle, combining the results of multiple sources at different sky locations and having different polarizations would permit a complete coverage of the CPT-even sector for each  $d$ , but at present the number of sources is insufficient for this. The above inequality can, however, be used to estimate the maximum sensitivity to



coefficients for Lorentz violation achieved by a given source. The depletion in polarization is largest when the light is in an equal admixture of the two normal modes,  $\Psi = \pm\pi/4$ . The effective degree of polarization then reduces to  $\Pi_{\text{eff}} = |\langle \cos \Phi \rangle|$ , which vanishes for relative rotations greater than  $\pi$  across an energy band. We can therefore estimate the maximal sensitivity to the CPT-even coefficients as

$$\left| \sum_{jm} {}_2Y_{jm}(\theta, \phi) (k_{(E)jm}^{(d)} + ik_{(B)jm}^{(d)}) \right| \lesssim \frac{\pi}{2|E_2^{d-3} - E_1^{d-3}|L^{(d)}}. \quad (10)$$

This result can be applied to the sources GRB 041219A, GRB 100826A, GRB 110301A, and GRB 110721A. For Lorentz-violating operators of dimensions  $d = 4, 6$ , and  $8$ , there are 10, 42, and 90 independent vacuum coefficients, respectively [10]. Table III lists the resulting constraints on a linear combination of these coefficients generated by each GRB. They represent sensitivities improved by factors of 10 to 100,000 over existing bounds on CPT-even violations of Lorentz invariance.

This work was supported in part by the Department of Energy under grant DE-FG02-91ER40661 and by the Indiana University Center for Spacetime Symmetries.

- 
- [1] A.A. Michelson and E.W. Morley, Am. J. Sci. **34**, 333 (1887); Phil. Mag. **24**, 449 (1887); R.J. Kennedy and E.M. Thorndike, Phys. Rev. **42**, 400 (1932); H.E. Ives and G.R. Stilwell, J. Opt. Soc. Am. **28**, 215 (1938).
  - [2] *Data Tables for Lorentz and CPT Violation, 2012 edition*, V.A. Kostelecký and N. Russell, arXiv:0801.0287v5.
  - [3] V.A. Kostelecký and S. Samuel, Phys. Rev. D **39**, 683 (1989); V.A. Kostelecký and R. Potting, Nucl. Phys. B **359**, 545 (1991).
  - [4] S. McGlynn *et al.*, Astron. Astrophys. **466**, 895 (2007); E. Kalemci, Astrophys. J. Suppl. **169**, 75 (2007).
  - [5] D. Yonetoku *et al.*, Astrophys. J. Lett. **743**, L30 (2011).
  - [6] D. Yonetoku *et al.*, Astrophys. J. Lett. **758**, L1 (2012).
  - [7] D. Colladay and V.A. Kostelecký, Phys. Rev. D **55**, 6760 (1997); Phys. Rev. D **58**, 116002 (1998); V.A. Kostelecký, Phys. Rev. D **69**, 105009 (2004).
  - [8] O.W. Greenberg, Phys. Rev. Lett. **89**, 231602 (2002).
  - [9] V.A. Kostelecký and R. Potting, Phys. Rev. D **51**, 3923 (1995).

- [10] V.A. Kostelecký and M. Mewes, Phys. Rev. D **80**, 015020 (2009).
- [11] V.A. Kostelecký and M. Mewes, Astrophys. J. Lett. **689**, L1 (2008).
- [12] V. Vasileiou, arXiv:1008.2913.
- [13] A.A. Abdo *et al.*, Science **323**, 1688 (2009).
- [14] D.R. Willis *et al.*, Astron. Astrophys. **439**, 245 (2005).
- [15] V.A. Kostelecký and M. Mewes, Phys. Rev. Lett. **97**, 140401 (2006).
- [16] F.W. Stecker, Astropart. Phys. **35**, 95 (2011).
- [17] P. Laurent *et al.*, Phys. Rev. D **83**, 121301(R) (2011).
- [18] K. Toma *et al.*, Phys. Rev. Lett. **109**, 241104 (2012).
- [19] W.S. Paciesas *et al.*, Astrophys. J. Suppl. **122**, 465 (1999).
- [20] W.T. Vestrand *et al.*, Nature **435**, 178 (2005).
- [21] K. Hurley *et al.*, GCN Circular No. 11156 (2010).
- [22] S. Foley, GCN Circular No. 11771 (2011).
- [23] V. Vasileiou *et al.*, GCN Circular No. 12188 (2011).
- [24] V.A. Kostelecký and M. Mewes, Phys. Rev. Lett. **87**, 251304 (2001); Phys. Rev. D **66**, 056005 (2002); Phys. Rev. Lett. **99**, 011601 (2007).
- [25] R.C. Myers and M. Pospelov, Phys. Rev. Lett. **90**, 211601 (2003).